Hypernetwork modeling and topology of high-order interactions for complex systems

Li Feng[1,2*], Huiying Gong[1,3*], Shen Zhang[4*], Xiang Liu[5,1], Yu Wang[1], Jincan Che[1,3], Ang Dong[1], Christopher H. Griffin[6], Claudia Gragnoli[7,8,9], Jie Wu[1], Shing-Tung Yau[1,4,10], and Rongling Wu[1,4,10]

[1]Beijing Institute of Mathematical Sciences and Applications, Beijing 101408, China
[2]Fisheries Engineering Institute, Chinese Academy of Fishery Sciences, Beijing 100141, China
[3]School of Grassland Science, Beijing Forestry University, Beijing 100083, China
[4]Qiuzhen College, Tsinghua University, Beijing 100084, China
[5]Department of Mathematics, Nankai University, Tianjin 300071, China
[6]Applied Research Laboratory, The Pennsylvania State University, University Park, PA 16802, USA
[7]Department of Public Health Sciences, Penn State College of Medicine, Hershey, PA 17033, USA
[8]Department of Medicine, Creighton University School of Medicine, Omaha, NE 68124, USA
[9]Molecular Biology Laboratory, Bios Biotech Multi-Diagnostic Health Center, Rome 00197, Italy
[10]Yau Mathematical Sciences Center, Tsinghua University, Beijing 100084, China

[*]These authors contributed to this work equally.

Correspondence to: Shing-Tung Yau, styau@tsinghua.edu.cn; Rongling Wu, ronglingwu@bimsa.cn

Significance

High-order interactions are a central element of complex systems, but existing network models mostly focus on pairwise interactions. We develop a generalized statistical mechanics model to reconstruct bidirectional, signed, and weighted hypernetworks that characterize how constituent agents are influenced by their own strategies, the strategies of co-existing agents, and strategies of interactions between other agents, as well as how directed pairwise interactions are influenced by individual agents. We use GLMY homology, a newly developed theory in algebraic topology, to dissect the topological architecture of hypernetworks in terms of nodes, links and hyperlinks. The integration of statistical mechanics and GLMY homology provides a generic tool for unveiling hidden patterns in complex systems across a wide spectrum of physical and biological scenarios.

Abstract

Interactions among the underlying agents of a complex system are not only limited to dyads, but can also occur in larger groups. Currently, no generic model has been developed to capture high-order interactions (HOI), which, along with pairwise interactions, portray a detailed landscape of complex systems. Here, we integrate evolutionary game theory and behavioral ecology into a unified statistical mechanics framework, allowing all agents (modeled as nodes) and their bidirectional, signed, and weighted interactions at various orders (modeled as links or hyperlinks) to be coded into hypernetworks. Such hypernetworks can distinguish between how pairwise interactions modulate a third agent (active HOI) and how the altered state of each agent in turn governs interactions between other agents (passive HOI). The simultaneous occurrence of active and passive HOI can drive complex systems to evolve at multiple time and space scales. We apply the model to reconstruct a hypernetwork of hexa-species microbial communities, and by dissecting the topological architecture of the hypernetwork using GLMY homology theory, we find distinct roles of pairwise interactions and HOI in shaping community behavior and dynamics. The statistical relevance of the hypernetwork model is validated using a series of *in vitro* mono-, co-, and tri-cultural experiments based on three bacterial species.

Keywords: pairwise interaction, high-order interaction, ecological community, evolutionary game theory, ecological behavior

Introduction

Complex systems are defined as those composed of large numbers of individual parts, which interact in such a way that the global behavior of the system, i.e., emergent properties, is not equal to the sum of the behavior of individual parts. An ecological community is an example of complex system, with a multitude of interspecies interactions ranging from mutualism to antagonism, and internal dynamics that underly the emergence of the communities[1,] community productivity, stability[2-4], and evolution across spatio-temporal scales[5-7]. However, existing models of complex systems assume relatively simple dyadic (pairwise) interactions[8-13], which, for ecological communities, means that the per capita effects of any one species on any other species are not dependent on the abundance of a tertiary species. This assumption is obviously violated by the omnipresent existence of HOI, where three or more parts act together as a subgroup to shape system behavior[9,14-26]. In the case of random interactions in ecological communities, the emergence of HOIs can alter the established relationship between diversity and stability[8], leading to new evolutionary trajectories[27,28].

In statistics, HOI are commonly defined as a deviation from the prediction of a null model, where only up to pairwise interactions are included[29]. Although this definition can test the presence/absence of HOI[30,31], it fails to characterize their mechanistic role in detail. A main challenge to proposing a quantitative, universally valid definition for HOI across different scenarios is that the relevance of interactions, exemplified by their multifaceted physical properties, are difficult to fully capture with existing theories[22,29]. For example, interspecies HOI are characteristic of their strength (how strongly two parts are linked), causality (directionality of the interaction), sign (whether one part exerts a favorable or detrimental effect on the other), and operating mode (whether the interaction between two parts affects, or is affected by, the presence of the others). In ecological studies, interspecific interactions are generally described and understood as the coarse-grained constitution of community behavior and stability[12,16,32]. We are motivated by a dynamics-based approach to chart the fine-grained details of interactions including HOI that operate in complex ecological communities.

Our model is mechanistic in the sense that it incorporates evolutionary game theory and behavioral ecology principles into a unified statistical mechanics framework. Interspecific interactions can be dynamically viewed as a game in which each species strives to maximize its payoff by applying an optimal strategy in response to the strategies of other species[33]. We expand this argument to decompose the abundance of a species into three components, one due to its intrinsic capacity, the

second resulting from the influence of other species on it, and the third from the influence of interactions between groups of other species on it. From an ecological perspective, one species interacts with another species in a way that is determined by how energy flows within the community[34]. The pattern of energy flow forms different types of interactions, including mutualism (both species benefit from each other), altruism (one species offers a benefit to the other, with no reward from the latter), aggression (one species is benefited at a cost to the second), and antagonism (two species compete against each other)[35]. More recently, we derived a series of biologically justified mathematical descriptors for each of these interaction types[36-38]. The combination of evolutionary game theory and behavioral ecology through dynamic equations creates a statistical mechanics model for defining a universal form of HOI and reconstructing hypernetworks filled with a full set of interaction characteristics at different orders. This model, in conjunction with GLMY homology theory, a topological theory of digraphs pioneered by S.-T. Yau and team[39-41], provides a generic tool to identify hidden patterns of community structure, organization and function at different levels of organization and across fields.

A statistical mechanic formalism of evolutionary game theory and behavioral ecology

Mixed interactive ordinary differential equations (miODE): Without loss of generality, we study complex systems by considering ecological communities of multiple species. Game-theoretic principles postulate that a species always strives to maximize its growth and fitness (payoff) by adopting an optimal strategy in response to the strategies of its conspecifics[42]. Evolutionary game theory extends the Nash equilibrium[43], at which no species can gain more payoff by merely changing its own strategy, to the notion of evolutionarily stable strategies (ESS)[44] and does not require a "rationality" assumption given that the payoff to the species (as a whole) changes as a result of the inherent dynamics of the system[45]. We derive a system of miODE's to characterize the dynamic change of strategies in the population[46]. Let $y_j(t)$ denote the abundance of species j ($j = 1, \dots, p$) observed at time t in a community of p species. The miODE of $y_j(t)$ is described as,

$$\frac{dy_j(t)}{dt} = Q_j\left(y_j(t)\right)$$

$$+\sum_{j'=1,j'\neq j}^{p} Q_{jj'}\left(y_{j'}(t)\right) \qquad \text{Pairwise interations}$$

$$+\sum_{j_1<j_2=2}^{p}\sum_{j_1=1}^{p} Q_{jj_1j_2}\left(z_{j_1j_2}(t)\right) \qquad \text{Active 3-way HOI}$$

$$+\sum_{j_2<j_3=3}^{p}\sum_{j_1<j_2=2}^{p}\sum_{j_1=1}^{p} Q_{jj_1j_2j_3}\left(z_{j_1j_2j_3}(t)\right) \qquad \text{Active 4-way HOI}$$

$$+\cdots$$

$$+\sum_{j_{p-2}<j_{p-1}=p-1}^{p}\ \cdots\ \sum_{j_1<j_2=2}^{p}\sum_{j_1=1}^{p} Q_{jj_1j_2\ldots j_{p-1}}\left(z_{j_1j_2\ldots j_{p-1}}(t)\right) \qquad \text{Active } p\text{-way HOI} \qquad (1)$$

where the first term of equation (1) at the right side quantifies the independent payoff (abundance) intrinsic to each species, the second term is the dependent payoff of this species arising from the influence of other species (expressed as directed pairwise interactions), the third term is the dependent payoff of this species due to the influence of pairwise interspecific interactions (expressed as directed 3-way HOI), the fourth term is the dependent payoff of this species due to the influence of 3-way interspecific interactions (expressed as directed 4-way HOI), and the last term is the dependent payoff of this species due to the influence of $(p-1)$-way interspecific interactions (expressed as directed p-way HOI). The third term and its subsequent terms characterize how higher-order interactions shape the emergent properties of the ecological community. As a first step of HOI modeling, we consider the first three terms of equation (1), where $Q_{j.}$ denotes the function of time-varying abundance of relevant species or time-varying pairwise interspecific interactions. We use a specific growth equation (see the Methods) to fit the independent abundance term and nonparametric Legendre Orthogonal Polynomials (LOP) to construct the dependent abundance terms that may have no explicit form.

Mathematical descriptors of ecological interactions: A critical issue is how to define the pairwise interactions, $z_{j_1j_2}(t)$ in equation (1), which are crucial for characterizing HOI. In ecological communities, while one species competes for resources with another species, these two species may also cooperate with each other through some shared materials[47] or substrate. Competition and cooperation are intertwined to determine community dynamics, implying that competition contains cooperation, whereas cooperation includes competition[34]. Thus, for any pair of co-existing species,

all possible types of ecological interactions, including mutualism, altruism, aggression, and antagonism, may be interchangeable and occur simultaneously in communities. We derived four mathematical descriptors for each type of interactions, expressed in a stationary status, based on animal behavioral ecology theory[36-38]. For example, two similar individuals in size, shape, and appearance tend to mutually cooperate[48], thus the mathematical descriptor of mutualism is expressed as the product of their corresponding trait values. The strength of mutualism is positively associated with this product given that the sum of the two values (i.e., useful resources) is fixed. The biological relevance of the mathematical descriptors has been validated by performing fish and microbial experiments[37,38]. The estimated $z_{j_1 j_2}(t)$ functions with forms taken from the mathematical descriptors are used to fit the third term of the miODE in equation (1), which describes how pairwise interactions influence the abundance of the third species, defined as active HOI.

As opposed to active HOI, there also exists a form of passive HOI, i.e., the influence of a species j' on the focal species j, denoted as $Q_{jj'}\left(y_{j'}(t)\right)$, is determined by the abundance of the third species, denoted as $y_{j''}(t)$ ($j'' = 1, \ldots, p; j'' \neq j' \neq j$). In a dyad community only composed of two species j and j'', $Q_{jj'}\left(y_{j'}(t)\right)$ is not affected by the third species, in which case $Q_{jj'}\left(y_{j'}(t)\right)$ is expressed as $Q^D_{jj'}\left(y_{j'}(t)\right)$. Thus, for a p-species community, we write $Q_{jj'}\left(y_{j'}(t)\right)$ as,

$$Q_{jj'}\left(y_{j'}(t)\right) = Q^D_{jj'}\left(y_{j'}(t)\right) + \sum_{j''=1, j''\neq j'\neq j}^{p} P_{(jj')j''}\left(y_{j''}(t)\right) \quad (2A)$$

$$= P_{jj'}\left(Q_{jj'}\left(y_{j'}(t)\right)\right) + \sum_{j''=1, j''\neq j'\neq j}^{p} P_{(jj')j''}\left(y_{j''}(t)\right) \quad (2B)$$

which suggests that $Q_{jj'}\left(y_{j'}(t)\right)$ in a multispecies community differs from $Q^D_{jj'}\left(y_{j'}(t)\right)$ by the second term in the right-hand side of equation (2A); i.e., the cumulative influence of species j'' on the directed effect of species j' on species j, specified as a function of $y_{j''}(t)$. Equation (2B) states that the directed pairwise interaction between species j and j' in a multi-species community is decomposed into two components, one being the independent pairwise interaction component that occurs under the assumption that no additional species is introduced, specified as a function of

$Q_{jj'}\left(y_{j'}(t)\right)$, and the other being the dependent interaction component that results from the influence of the third species j'' on the j-j'pairwise interaction. The dependent interaction component is called passive HOI. It is also possible that active HOI in the hexad is determined by the third species, forming a higher-order passive HOI, which is mathematically expressed as

$$\begin{aligned} Q_{jj_1j_2}\left(z_{j_1j_2}(t)\right) &= Q^{D}_{jj_1j_2}\left(z_{j_1j_2}(t)\right) + \Sigma^{p}_{j''=1,j''\neq j_1\neq j_2\neq j} P_{(jj_1j_2)j''}(y_{j''}(t)) \\ &= P_{jj'}\left(Q_{jj_1j_2}\left(z_{j_1j_2}(t)\right)\right) + \sum_{j''=1,j''\neq j_1\neq j_2\neq j}^{p} P_{(jj_1j_2)j''}\left(y_{j''}(t)\right) \end{aligned} \quad (3)$$

where the first term represents an independent active three-way HOI, i.e., one that occurs under the assumption of the additional fourth species and the second term is four-way passive HOI, i.e., the influence of the third species on the active HOI. Independent and dependent interaction components involved in equations (2) and (3) may have no explicit form, but they can be smoothened by LOP.

The combination of equations (1) – (3) establishes the mathematical basis of our statistical mechanics model for characterizing both active and passive HOI. Indeed, they can not only fully capture the emergent properties of interactions, but also represent a group of recursive equations, by which the evolutionary trajectories of complex systems, driven by HOI, can be traced.

Disentangling microbial HOI organization: To validate the power of our miODE model to reveal HOI at any order, we reanalyze a hexa-cultured bacterial species dataset collected in Hu et al.'s ecological study[34]. Any species in a six-species S1-S2-S3-S4-S5-S6 community is affected by five co-existing species, 10 pairwise interspecific interactions, six three-way interspecific interactions, three four-way interspecific interactions, and one six-way interspecific interaction. The six species are grouped into two triads S1-S2-S3 and S4-S5-S6, which are tri-cultured, respectively. In bacterial communities, four types of interactions, whose strength can be calculated using our mathematical descriptors[38], may occur simultaneously. Assuming that a bacterial community starts from mutualism, we build a group of miODE to estimate and code the independent components of each species as nodes and the dependent components due to different orders of interspecific interactions as links or hyperlinks into hypernetworks.

Figure 1 illustrates part of the hypernetwork of the hexa-species mutualistic community, covering directed pairwise interactions, directed three-way active HOI, and directed four-way passive HOI. We find that all mutualistic relationships assumed to occur in the original community (Fig, 1A) become antagonistic or aggressive/altruistic under active HOI's (Fig. 1B1). For example, active HOI drive the S1-S2 interaction from mutualistic to antagonistic, whereas without active HOI, S1 and S5 are mutually cooperative, but with active HOI, S1 starts to repress S5 although S5 still promotes S1. Mutualism between any pair of species affects the abundance of the third species, however to different extents and with different signs (Fig. 1B2). While mutualism between S2 and S3, S2 and S5, S3 and S5, S3 and S6, and S5 and S6 promotes the abundance of S1, mutualism between S2 and S4, S2 and S6, S3 and S4, S4 and S5, and S4 and S6 inhibits the abundance of S1. The pattern and sign of such active HOI's on the abundance of the other species are detailed in the hypernetwork (Fig. 1B2).

The impact of active HOI in a group of three species is quickly influenced by the fourth species through passive HOI (Fig. 1C). The degree to which S2-S3 mutualism inhibits the abundance of S1 is negatively regulated by S4 and S6 but positively regulated by S5 to a larger extent. We find that S5 also promotes the active HOI of S1-S3 mutualism on S2 and the active HOI of S1-S2 mutualism on S3. The detailed pattern of the role of passive HOI in mediating hypernetwork structure can be seen from Fig. 1C. We reconstruct hypernetworks for two triads S1-S2-S3 and S4-S5-S6, from which to chart the decomposition curves of each species, in comparison with those in the hexad (Fig. 2). In triad S1-S2-S3, the abundance level of S1 is influenced by its coexisting S2 (in a negative sign) and S3 (in a positive sign) and their mutualism (in a negative sign). The negative cumulative effect of these influences compromises the independent abundance of S1, making its observed abundance reduced. In the hexad, the abundance of S1 is affected not only by the abundance of S2 – S6 but also by pairwise interspecific interactions among these species. We find that the influence of S2 and S3 on S1 differs in the hexad than in the triad S1-S2-S3 possibly because of the existence of additional species S4-S6. For the same reason, the influence of the S2-S3 interaction on S1 changes from the triad to the hexad. The abundance of the other species in the hexad is also affected by co-existing species and their interspecific interactions, but with the pattern and extent differing dramatically from the those observed in the triads (Fig. 2).

Why does the influence of one species on its co-existing species changes when new species are added to the community? This can be explained by passive HOI, i.e., the influence of additional species on the independent component. We have identified the existence of passive HOI (Fig. 1), and

using equation (3), we characterize how active HOI are determined by additional species (Fig. 3). In the hexad, the influence of the S2-S3 interaction on S1 (expressed as S2S3→S1) is consistently small over time, but this influence is virtually very large in the S1-S2-S3 triad (no additional species). This difference can be explained to be due to the negative regulation of this active HOI by S4 and S6, despite with a much smaller positive regulation by S5. Four-way passive HOI are compromised due to the latter three species, shifting the active HOI from negative to slightly positive. We also identify a striking four-way passive HOI that affects active HOI involving S2 – S6, respectively (Fig. 3). It is interesting to see that independent active HOI for each species estimated from the hexad data under the assumption of no additional species are broadly in agreement with those observed in the triads, suggesting that the mixed ODE of equation (3) is biologically relevant and justifiable.

GLMY homology dissection of hypernetworks

The 6-node microbial hypernetwork, reconstructed by equations (1) – (3), is composed of pairwise interactions, 3-way active HOI, and 4-way passive HOI. We develop and apply the GLMY theory to dissect the topological architecture of this hypernetwork based on positive interactions, negative interactions and a mix of positive and negative interactions (Fig. 4A). We identify the 2-dimensional cycles (holes) in positive and negative hypernetworks, showing their architectural complexity. The hypernetwork architecture is especially complex, with 2-, 3-, and 4-dimensional homological features, when both positive and negative interactions are considered. This complexity is mainly derived from the existence of HOI. Three sets of 3-way active HOI among S4, S5, and S6 form 3-dimensional homological features (voids) (Fig. 4B). There are four 4-dimensional homological features each produced by four sets of four-way passive HOI involving five species, with the first homological feature composed of S1, S2, S3, S4, and S5, the second composed of S1, S2, S4, S5, and S6, the third composed of S1, S3, S4, S5, and S6, and the fourth composed of S1, S3, S4, S5, and S6. Note that no 3- and 4-dimensional homological features are formed purely based on positive or negative interactions.

We further analyze the GLMY persistent homology of the microbial hypernetwork based on the order of interspecific interactions (Fig. S1). Both positive and negative interactions occur pairwise, among three species, and among four species. At dimension 1, we identify five positive-driven homological features for pairwise interactions (composed of S1, S3, S4, S5, and S6), with one

subnetwork (corresponding to dimension 1) being persistent, suggesting that the sub-networks of pairwise interactions (excluding S2) converge into one network as a whole (Fig. S1) with a single one-dimensional network. At dimension 2, we also identify five positive-driven homological features for pairwise interactions at a higher level of complexity, derived from {S5→S4, S4→S3, S5→S3}, {S4→S5, S4→S3, S5→S3}, {S6→S3, S6→S5, S5→S3}, {S6→S3, S4→S6, S4→S3}, and {S6→S3, S5→S6, S5→S3}. At dimension 2, we identify two positive-driven homological features for 3-way interactions, corresponding to two sub-networks S4-S6 and S5 of {(S4-S6)→S5}. For 4-way positive interactions, we identify five 1-dimensional homological features, corresponding to S5, S6, {(S4-S6)→S5}, S1, S3, respectively, the first three of which become three persistent independent networks, and one 2-dimensional homological feature from {S1→{(S4-S6)→S5} and {S3→{(S4-S6)→S5}. We can also identify homological features at different dimensions based on negative networks (Fig. S1) and mixed positive and negative networks (Fig. S1).

We calculate persistent 2-layer homological features of sub-hypernetworks for each species based on positive, negative and mixed positive and negative interactions (Fig. S2). For negative hypernetworks, we identify no 1-dimensional homological features for species 2, two for species S1 and S4, three for species S5 and S6, and four for species S3 (Fig. S2A). For positive hypernetworks, we identify two 1-dimensional homological features for species S3, four for species S5 and S6, five for species S1 and S4, and six for species S2 (Fig. S2B). As can be seen, both positive and negative 1-dimensional homological features divide the six species into four groups, S1 and S4, S2, S3, and S5 and S6. These four groups differ in the complexity of their positive and negative hypernetworks. Except for S2, all species converge in 1-dimensional homological features into one single subnetwork.

Experimental validation of statistical hypernetworks

Ecological experiment of microbial culture: We design and conduct an ecological experiment to validate the biological value of the model. We randomly match three bacterial strains each from a different species, *Escherichia coli* (E), *Staphylococcus aureus* (S), and *Pseudomonas aeruginosa* (P), and mix-culture them in a medium-loaded flask. We obtain and grow 100 such unrelated E-S-P triads. We use our statistical hypernetwork model to estimate and code the independent component, first-order dependent component (due to individual species) and second-order dependent component (due to interspecific interactions) into bidirectional, sign, and weighted hypernetworks for each triad

(see Fig. 5A for an example from a triad composed of CYH-D12 from E, CYH-S12 from S, and CYH-P13 from P). In a mutualistic community, the cooperation of any pair of species would seriously affect the growth of the third species (active HOI, $P < 0.05$). For example, cooperation between species S and P consistently promotes species E during all phases of growth, whereas the cooperation between species E and P and between species E and S may promote or inhibit the third species, depending on the phase of growth (Fig. 5B). We also find that antagonism, altruism, and aggression influence the growth of the third species, although the sign and strength of active HOIs vary from case to case. In all situations, active HOI cyclically change in strength and/or sign over time, suggesting that they play a role in adjusting community stability and dynamics.

Active HOI not only affect community growth, but also bring about dramatic changes in interaction structure within communities. Active HOI shift the mutualism of species E with S and P to altruism/aggression, with S and P inhibiting E but E promoting S and P (to a lesser extent), driving species S and P from mutualism to amensalism; i.e., P inhibits S but S has a trivial influence on P (Fig. 5B). Because of the collective effects of active HOI and altered pairwise interaction patterns, species E and S display reduced growth compared to their independent growth, whereas species P increases its growth when it relocates from a socially isolated environment to a socialized environment (Fig. 5B). Strong active HOI and their influences on pairwise interactions are also detected when the communities are filled with antagonistic, altruistic or aggressive interactions (Fig. 5B).

We further characterize how newly formed directed interactions due to active HOI are affected by the growth of the third species (passive HOI). In a triad, species P influences the interaction between E and S, but in different ways depending on whether S affects E or E affects S (Fig. 5C). The inhibition of species E by S is strengthened by species P since this inhibition is stronger when P co-exists with E and S than when P is assumed to be absent. The influence of species P on the promotion of S by E changes its sign during ecological time; in the first 8-9 hours, this influence is negative whereas it becomes increasingly positive after this time, making the influence of E on S sharply different between cases with P and without P.

It is interesting to note that species S obstructs both the inhibition of P for E and the promotion of E for P, making the negative impact (predation) of P on E, as seen in the dyad, much smaller in extent (Fig. 5C). The influence of the same species E on the inhibition of S by P and the semi-inhibition of P by S is very different, which leads to distinct patterns of dyadic S-P interactions in the triad.

Likewise, we can also illustrate the pattern of how pairwise interactions are altered by active HOI to form various passive HOI patterns, initiated from antagonism, altruism, and aggression in the community (Fig. 5C).

Model validation: The central theme of our model is to divide the growth of a species in a social community (i.e., community growth) into its independent and dependent components. The independent component is this species' growth (fitted by a growth equation) that is supposed to be expressed in isolation (isolation growth), whereas the dependent component, i.e., the deviation of community growth from independent growth, reflects the extent to which this species is influenced by its co-existing species. If our model is logically correct, then the independent component estimated from it should be consistent with isolated growth. We perform an additional experiment to cultivate individual strains from each species in socially isolated monocultures (singletons) and individual strain pairs each from a different species in socialized co-cultures (dyads).

Figure 6A illustrates the goodness-of-fit of the growth equation (4) for isolation growth data for each species at different time points in monoculture. We find that the independent growth curve of a pair of species estimated from a dyad is in remarkable agreement with the isolation growth curve from their corresponding singletons (Fig. 6A). For example, the growth trajectory of species E from a singleton can well be approximated by its independent growth trajectories from dyads E-S and E-P. We also find that the independent growth curves of each species from a triad are consistent with their respective isolation growth curves, even if different types of pairwise interactions are initially assumed (Fig. 6B). These two types of consistency hold for all triads. Taken together, our model that decomposes community growth into independent and dependent components in accordance with evolutionary game theory is logically reasonable and powerful.

The directed interaction between two species estimated from a triad includes the independent interaction component that occurs when these two species are assumed not to co-exist with any other species and the dependent interaction component due to the influence on this interaction by the third species. Thus, if the independent component estimated from the triad is consistent with the dependent component estimated from the corresponding dyad, then this suggests that our model can be biologically justified. As illustrated in Fig. 6C, all six possible directed interactions under each type of pairwise interactions exhibit such consistency, confirming the relevance and robustness of our statistical hypernetwork model.

Discussion

The pervasive occurrence of nonlinear interactions at various orders as a fundamental ingredient of complex systems has fostered an increasing interest in reconstructing hypernetworks that are encapsulated by nodes, links, and hyperlinks. In the field of ecological communities, both empirical and theoretical studies show that the introduction of HOI gives rise to new emergent physical phenomena, which cannot be understood by limiting the analysis of structured properties to simple low-order dyads[7,12,14,15,49-52]. In this article, we propose a universal statistical hypernetwork theory to define, quantify, and estimate complex HOI. This theory, derived from the interdisciplinary combination of evolutionary game theory and behavioral ecology, can leverage existing pairwise interaction models to include HOI at any order and expand their applications to complex communities.

Currently, most networks inferred from complex systems, such as gene regulatory networks, metabolic networks, and ecological networks, are co-occurrence networks or probabilistic networks, in which the links of different agents are identified without capturing their full properties, including causality, sign, strength, and feedback cycle. We attempt to circumvent these drawbacks by viewing agent-agent interactions as an evolving game. Evolutionary game theory decomposes the abundance of individual agents into their independent and dependent components which are distinguished from one another by miODE models[36,46], whose asymptotic properties have been found and proved[53]. We encode independent components of individual agents as nodes, the first-order dependent components of individual agent pairs as links, and the high-order dependent components of individual agent sets (containing more than two agents) as hyperlinks to construct bidirectional, signed, and weighted hypernetworks. Thus, compared to existing models, our hypernetwork model should be more effective for studying the topological architecture and functionality of interspecies interactions that underlie community behavior.

We postulate that a community evolves along eco-evolutionary times, starting from state 1, constituted by pairwise interactions (Fig. 7). As predicted by equation (1), the emergence of active HOI will lead to various changes in the growth dynamics of each species, implying that all species are reshuffled, and the dynamics move towards state 2, in which community diversity and interaction differ from that in state 1. The altered growth of each species will in turn affect how the other two species interact with each other, a phenomenon called passive HOI. A passive HOI can be explained

as the alteration of any directed interactions occurring in a species-rich community when compared to those in a comparatively species-poor community, resulting from the additional species and their resulting interactions. Driven by passive HOI, the growth of individual species will change again, moving the community to state 3 (Fig. 7). The process of state transition continues, forming a driving force for community dynamics and evolution, which can be predicted by the statistical mechanics model composed of recursive HOI equations (1) – (3). We mathematically proved that the emergence of HOI can lead to the creation of a subcritical Hopf bifurcation and consequently an unstable limit cycle, a kind of behavior that cannot occur in pairwise replicators[27,28].

One of the most salient parts of our study lies in the seamless integration of hypernetworks and GLMY homology theory[39-41]. GLMY theory has proven to be powerful for dissecting the topology of digraphs, and its application to the analysis of real data has provided new insights into the mechanisms underlying molecular interactions[54,55] and metabolic interaction-driven human diseases[56]. In this study, we leverage GLMY theory to reveal the topological architecture of hypernetworks, under which a fundamental question of how HOI play a distinctive role from pairwise interactions in mediating the emergent behavior of complex systems can be addressed. We argue that the GMLY dissection of hypernetworks should become an essential procedure for dissecting extremely complex communities, such as the gut microbiota[57] because these systems include an enormous number of pairwise and and higher-order interactions at various orders.

Reconstructing hypernetworks may encounter computational burden when considering a large number of entities. We circumvent this issue by classifying these entities into distinct modules, in each of which entities are connected more tightly with each other than with those from other modules. If the number of entities within a module is still large, we further classify this module into distinct submodules. This process of classification may repeat until the number of entities within a unit follows Dunbar's number, the maximum size of social groups in which each individual can establish a stable social relationship with every other individual[58]. It is computationally feasible to reconstruct hypernetworks from Dunbar's number of entities.

Many coarse-grained approaches attempt to study community behavior by formulating a few key parameters, such as the number of species and the distribution of pairwise interaction strength. Alternatively, the theory proposed in this article is based on fine-grained thinking and can characterize the detailed internal workings and functionality of complex systems at multiple levels of interaction. To our knowledge, our theory is among the first to systematically map and model how

the collective actions of individual agents through physical laws could explain and predict state transition in complex systems. This theory may find immediate implications for unveiling general principles underlying a range of biological processes from macroscopic ecosystems to microscopic cellular and molecule circuits.

Materials and Methods

Bacterial *in vitro* culture experiment. We collected 100 bacterial strains of each species, *Escherichia coli* (E), *Staphylococcus aureus* (S), and *Pseudomonas aeruginosa* (P), from the National Infrastructure of Microbial Resources, China. These strains were pre-cultivated with a procedure as described in He et al.[59]. The cultural experiment includes 300 monocultures for each strain, 300 co-cultures for each pair of strains (dyad) in a 1:1 ratio, each from a different species, and 100 tri-cultures for each set of three strains (triad) in a 1:1:1 ratio, each from a different species. To assure the independence of dyads and triads, none of the same strains were used in any two co-cultures or any two tri-cultures. All cultures were taken in flasks of the same size, filled with 25 mL of two-times diluted brain heart infusion medium (OXOID, Basingstoke, England). The flasks were incubated at 30 °C and shaken at 130 rpm.

Each strain in flasks was sampled once every 0.5 h during the first 2 h of cultivation, followed by once every 2 h after 2 h and once every 4 h after 12 h, with a total culture period of 36 h. Quantitative PCR (qPCR) measurements of *E. coli* and *S. aureus* were performed according to the previous protocol[31]. To detect *P. aeruginosa* strains, 159 bp of the gyrA gene encoding DNA gyrase subunit A were amplified by forward primer CAAGCCCTACAAGAAATCCG and reverse primer TCCACCGAACCGAAGTTG. The qPCR counts of each strain at a time point, averaged over three replicates, were used as the time-varying abundance level of this strain.

In joint-cultural experiments of different strains from bacterial species isolated from terrestrial environments, Hu et al.[32] measured abundance levels of each species at the end of each of 10 daily cycles during growth. To generalize our model to more complex communities, we chose their eight hex-cultures of six different species grown in low nutrient concentrations to analyze HOI, in comparison with the same HOI in the tri-cultures using three of these six species. The procedures of sampling and inoculating these strains are described in ref 30.

Modeling microbial growth. The growth of a microbial species in a monoculture does not depends on the influence of any other species. Let $y_j(t)$ denote the growth of a strain from a species *j* in the monoculture at time *t* ($1, \dots, p$; $t = t_1, \dots, t_T$). We model the growth trajectory of the strain by a logistic equation[60], expressed as,

$$\frac{dy_j(t)}{dt} = \alpha_j y_j(t) \left(1 - \frac{y_j(t)}{K_j}\right)^{\lambda_j} \tag{4}$$

where α_j is the growth rate of a species *j* in the absence of limited resources, K_j is the carrying capacity of a species, i.e., the asymptotic growth this species can achieve, and λ_j is the exponent that describes how quickly the species reaches the asymptotic growth. We use this growth equation to fit the independent growth $Q_j\left(y_j(t)\right)$ of the miODE in equation (1), which represents the virtual growth of strain j in the hexa-culture under the assumption of no influence from any co-existing species. This equation is also used to model the independent growth of strain j in the co-culture and tri-culture.

Solving miODEs. Consider a *p*-species community in which the abundance of each species *j* ($j = 1, \dots, p$) is measured at a series of time points ($t_1, \dots, t_T$), denoted as $\boldsymbol{y}_j = (y_j(t_1), \dots, y_j(t_T))$. The likelihood of time-varying abundance of all three species is formulated as,

$$L_1(\boldsymbol{y}) = f\left(\boldsymbol{y}_1, \dots, \boldsymbol{y}_p : \boldsymbol{\mu}_1, \dots, \boldsymbol{\mu}_p; \boldsymbol{\Sigma}\right) \tag{5}$$

where $f(\cdot)$ is a multivariate longitudinal normal density probability function with time-varying mean vector,

$$\boldsymbol{\mu} = (\boldsymbol{\mu}_1, \dots, \boldsymbol{\mu}_p) = \left(\mu_1(t_1), \dots, \mu_1(t_T), \dots, \mu_p(t_1), \dots, \mu_p(t_T)\right) \tag{6}$$

and time-varying covariance matrix,

$$\boldsymbol{\Sigma} = \begin{pmatrix} \boldsymbol{\Sigma}_1 & \cdots & \boldsymbol{\Sigma}_{1p} \\ \vdots & \ddots & \vdots \\ \boldsymbol{\Sigma}_{p1} & \cdots & \boldsymbol{\Sigma}_p \end{pmatrix} \tag{7}$$

with $\mathbf{\Sigma}_j$ on diagonal being a ($T \times T$)-covariance matrix for species j and $\mathbf{\Sigma}_{jj'}$ off diagonal being a ($T \times T$)-covariance matrix among species j and species j' ($j < j' = 1, \ldots, p$).

We integrate miODEs to model the mean vector of equation (6) and the first-order structured antedependent (SAD(1)) process[61,62] to model the autocorrelative structure of the matrix in equation (7). We implemented a fourth-order Runge-Kutta algorithm for miODE solving while maximizing the likelihood function (5). The maximum likelihood estimates (MLE) of the independent and dependent components are encoded into weighted mathematical graphs as a network dissection of the ecological communities.

Data and code availability. The datasets generated in this study are available from the corresponding authors on reasonable request. The code used for all analyses in this study is available on GitHub (https://github.com/CCB-HyperNetwork). All other code is available on reasonable request.

Acknowledgements. We thank many members at the Center for Computational Biology, Beijing Forestry University, for their contributions to this work at different stages. This support was partially supported by the Start-up Fund at Beijing Institute of Mathematical Sciences and Applications. CG was supported in part by the US National Science Foundation under grant DMS-1814876 and CMMI-1932991.

Author contributions. LF, HG, SZ, YW, CW conducted data analysis, reconstructed hypernetworks, and wrote computer programs. XL, SZ, JW performed GLMY analysis. CHG studied high-order interaction architectures. S-TY provided original GLMY theory and supervised the project. RW conceived of idea and wrote the manuscript with inputs from other authors.

Competing interests. The authors declare no competing interests.

1 F. A. Gorter *et al*., Understanding the evolution of interspecies interactions in microbial communities. *Phil. Trans. R. Soc. B*. **375**, 20190256 (2020).

2 C. Ratzke *et al*., Strength of species interactions determines biodiversity and stability in microbial communities. *Nat. Ecol. Evol.* **4**, 376-383 (2020).

3 A. Omidi *et al*., Reviewing interspecies interactions as a driving force affecting the community structure in lakes via cyanotoxins. *Microorganisms*. **9**, 1583 (2021).

4 S. E. Wuest *et al*., Ecological and evolutionary approaches to improving crop variety mixtures. *Nat. Ecol. Evol*. **5**, 1068-1077 (2021).

5 A. Swain *et al*., Higher-order effects, continuous species interactions, and trait evolution shape microbial spatial dynamics. *Proc. Natl. Acad. Sci. U. S. A.* **119**, e2020956119 (2022).

6 T. G. Barraclough *et al*., How do species interactions affect evolutionary dynamics across whole communities? *Ann. Rev. Ecol. Evol. Syst.* **46**, 25-48 (2015).

7 A. Åkesson *et al*., The importance of species interactions in eco-evolutionary community dynamics under climate change. *Nat. Commun.* **12**, 4759 (2021).

8 R. M. May *et al*., Will a large complex system be stable? *Nature* **238**, 413-414 (1972).

9 M. J. Pomerantz *et al*., Do "higher order interactions" in competition systems really exist? *Am. Nat.* **117**, 583-591 (1981).

10 R. A. Relyea *et al*., Predicting community outcomes from pairwise interactions: integrating density- and trait-mediated effects. *Oecologia*. **131**, 569-579 (2002).

11 S. M. Kodera *et al*., Conceptual strategies for characterizing interactions in microbial communities. *iScience.* **25**, 103775 (2022).

12 S. Allesina *et al*., The stability–complexity relationship at age 40: a random matrix perspective. *Popul. Ecol.* **57**, 63-75 (2015).

13 M.Vellend, The theory of ecological communities. (Princeton University Press, NJ, 2016).

14 A. R. Kleinhesselink *et al*., Levine JM Detecting and interpreting higher-order interactions in ecological communities. *Ecol. Lett.* **25**, 1604-1617 (2022).

15 J. M. Levine *et al*., Beyond pairwise mechanisms of species coexistence in complex communities. *Nature* **546**, 56-64 (2017).

16 J. Grilli *et al*., Higher-order interactions stabilize dynamics in competitive network models. *Nature* **548**, 210-213 (2017).

17 E. Bairey *et al*., High-order species interactions shape ecosystem diversity. *Nat. Commun.* **7**, 12285-12285 (2016).

18 D. McClean *et al*., Coping with multiple enemies: pairwise interactions do not predict evolutionary change in complex multitrophic communities. *Oikos.* **128**, 1588-1599 (2019).

19 P. Skardal *et al*., Higher-order interactions can better optimize network synchronization. *Phys. Rev. Res.* **3**, 043193 (2021).

20 T. Gibbs *et al*., Coexistence in diverse communities with higher-order interactions. .*Proc Natl Acad Sci U. S. A.* **119**, e2205063119 (2022).

21 F. Battiston *et al*., The physics of higher-order interactions in complex systems. *Nat. Phys.* **17**, 1093-1098 (2021).

22 F. Battiston *et al*., Networks beyond pairwise interactions: Structure and dynamics, *Phys. Rep.* **874**, 1-92 (2020),

23 R. Lambiotte *et al*., From networks to optimal higher-order models of complex systems. *Nat. Phys.* **15**, 313-320 (2019).

24 M. M. Mayfield *et al*., Higher-order interactions capture unexplained complexity in diverse communities. *Nat Ecol Evol.* **1**, 62 (2017).

25 H. Mickalide *et al*., Higher-Order Interaction between Species Inhibits Bacterial Invasion of a Phototroph-Predator Microbial Community. *Cell Syst.* **9**, 521-533 (2019).

26 J. Deng *et al*., Understanding the impact of third-party species on pairwise coexistence. *PLoS Comput. Biol.* **18**, e1010630 (2022).

27 C. Griffin *et al*., Higher-order dynamics in the replicator equation produce a limit cycle in rock-paper-scissors. *EPL*. **142**, 33001 (2023).

28 C. Griffin *et al*., Spatial dynamics of higher order rock-paper-scissors and generalisations. *J. Phys. A-Math. Theor*. **57**, 185701 (2024).

29 A. Sanchez, Defining Higher-Order Interactions in Synthetic Ecology: Lessons from Physics and Quantitative Genetics. *Cell Syst.* **9**, 519-520 (2019).

30 D. M. Weinreich *et al*., Should evolutionary geneticists worry about higher-order epistasis? *Curr. Opin. Genet. Dev.* **23**, 700-707 (2013).

31 E. Tekin *et al*., General form for interaction measures and framework for deriving higher-order emergent effects. *Front. Ecol. Evol.* **6**, 166 (2018).

32 J. Hu *et al*., Emergent phases of ecological diversity and dynamics mapped in microcosms. *Science* **378**, 85-89 (2022).

33 J. Liu *et al*., Inferring ecosystem networks as information flows. *Sci Rep*. **11**, 7094 (2021).

34 N. P. Moran *et al*., Shifts between cooperation and antagonism driven by individual variation: A systematic synthesis review. *Oikos*. https://doi.org/10.1111/oik.08201. (2022).

35 R. L. Wu *et al*., Recovering dynamic networks in big static datasets. *Phys. Rep.* **917**, 1-59 (2021).

36 L. Jiang *et al*., A mapping framework of competition–cooperation QTLs that drive community dynamics. *Nat. Commun*. **9**, 3010 (2018).

37 L. Jiang *et al*., A behavioral model for mapping the genetic architecture of gut-microbiota networks. *Gut. Microbes.* **13**, 1820847 (2021).

38 S. Wu *et al*., A quantitative decision theory of animal conflict. *Heliyon*. **7**, e07621 (2021).

39 A. Grigor'yan *et al*., Homologies of path complexes and digraphs. *arXiv*:**1207**, 2834v4 (2013).

40 A. Grigor'yan *et al*., Homotopy theory for digraphs. *Pure Appl. Math. Quart.* **10**, 619-674 (2014).

41 A. Grigor'yan *et al*., Path complexes and their homologies. *J. Math. Sci.* **248**, 564-599 (2020).

42 J. von Neumann *et al*., Theory of Games and Economic Behavior. (Princeton University Press, Princeton, 1944).

43 J. F. Nash, Equilibrium points in n-person games. *Proc. Natl. Acad. Sci. U. S. A.* **36**, 48-49 (1950).

44 J. M. M. Smith *et al*., Logic of animal conflict. *Nature* **246**, 15-18 (1973).

45 C. C. Cowden *et al*., Game theory, evolutionary stable strategies and the evolution of biological interactions. *Nat. Ed. Knowledge.* **3**, 6 (2012).

46 L. D. Sun *et al*., Statistical mechanics of clock gene networks underlying circadian rhythms. *Appl Phys Rev.* **8**, 021313 (2020).

47 F. Pinotti *et al*., Interplay between competitive and cooperative interactions in a three-player pathogen system. *R. Soc. Open Sci.* **7**, 190305 (2020).

48 T. Antal *et al*., Evolution of cooperation by phenotypic similarity. *Proc Natl Acad Sci U. S. A.* **106**, 8597-600 (2009).

49 T. G. Whitham *et al*., Intraspecific Genetic Variation and Species Interactions Contribute to Community Evolution. *Ann Rev Ecol Evol Syst.* **51**, 587-612 (2020).

50 P. A. Abrams, Arguments in favor of higher order interactions. *Am. Nat.* **121**, 887-891 (1983).

51 D. S. Wilson, Complex Interactions in Metacommunities, with Implications for Biodiversity and Higher Levels of Selection. *Ecology*. **73**, 1984-2000 (1992).

52 A. D. Letten *et al*., The mechanistic basis for higher-order interactions and non-additivity in competitive communities. *Ecol. Lett.* **22**, 423-436 (2019).

53 C. Griffin *et al*., Analysis of quasi-dynamic ordinary differential equations and the quasi-dynamic replicator. *Physica A*. **555**, 124422 (2019).

54 D. Chen *et al*., Path Topology in Molecular and Materials Sciences. *J Phys Chem Lett.* **14**, 954-964 (2023).

55 S. Chowdhury *et al*., Persistent path homology of directed networks. (SODA '18: Proceedings of the Twenty-Ninth Annual ACM-SIAM Symposium on Discrete Algorithms, 2018).

56 S. Wu *et al*., The metabolomic physics of complex diseases. *PNAS*. **120**, e2308496120 (2023).

57 W. Kong *et al*., Designing microbial consortia with defined social interactions. *Nat. Chem. Biol.* **14**, 821-829 (2018).

58 R. I. M. Dunbar, Neocortex size as a constraint on group size in primates. *J Hum Evol*. **22** (6): 469-493 (1992).

59 X. He *et al*., Bacterial genetic architecture of ecological interactions in co-culture by GWAS-taking *Escherichia coli* and *Staphylococcus aureus* as an example. *Front Microbiol*. **8**, 2332 (2017).

60 M. Kumar *et al*., Modelling approaches for studying the microbiome. *Nat Microbiol.* **4**, 1253-1267 (2019).

61 W. Zhao *et al*., A non-stationary model for functional mapping of complex traits. *Bioinformatics*. **21**, 2469-2477 (2005).

62 W. Zhao *et al*., Structured antedependence models for functional mapping of multivariate longitudinal traits. *Stat. Methods Mol.* **4**, 1544-6115 (2005).

Figure Legends

Figure 1 State change a hexad hypernetwork. (**A**) State 1 in which six species (S1- S6) are assumed to cooperatively interact with each other to form a six-node mutualistic network. Grey bidirectional arrows represent the mutualism between a pair of species, with the thickness of lines proportional to the strength of mutualism. (**B**) Interactions operate in the six-species community both in a dyadic manner (B1) and through active HOI (B2). Each species (indicated by an ellipse) is promoted (red line) or inhibited (blue line) by every other species and every possible pair of species involving no focal species, moving the community towards state 2. Plus represents the simultaneous occurrence of all these interactions with a focal species in the community. (**C**) Altered abundance in a species promotes (red line) or inhibits (blue line) the active HOI to produce a four-way passive HOI by which the community enters state 3. In each case, the thickness of lines is proportional to the strength of the active or passive HOI. Note that only those high-order passive HOI that act on the active HOI, which can also be observed in triads S1-S2-S3 and S4-S5-S6, are shown.

Figure 2 Abundance trajectory of each species (S1-S6) fitted by observed data (blue dots) from a hexad S1-S2-S3-S4-S5-S6 and two triads S1-S2-S3 and S4-S5-S6. This fitted trajectory of each species is decomposed into its independent growth curve (red line), first-order independent growth curves (green line) due to the influence on this focal species by the other five species, and second-order dependent growth curves (orange line) due to the influence on this focal species of pairwise mutualism among the other five species. At two sides of the hexad curves are the abundance trajectory of each species (blue line) fitted by observed data (blue dots) from triads S1-S2-S3 and S4-S5-S6, respectively. The fitted trajectory of a species in the triad is decomposed into its independent growth curve (red line), first-order dependent growth curve (green line) due to the influence of the other two species on this focal species, and second-order dependent growth curves (orange line) due to the influence on this focal species of the mutualism between the other two species. For comparison, the same type of the second-order dependent growth curves is indicated between the hexad and triads.

Figure 3 The detection of high-order passive HOI from a hexad S1-S2-S3-S4-S5-S6. The trajectory of the active HOI (blue line) involving a set of three species from triad S1-S2-S3 (**A**) and S4-S5-S6 (**B**), fitted by time-dependent estimation values (blue dots) from the hexad data, is decomposed into its independent component that is assumed to occur in a condition without the

existence of any additional species (red line) and dependent components arising from the existence of additional species (green line). The broken line represents the trajectory of the active HOI detected in a triad (with no fourth species in this case), whose consistency with the above independent component estimated from the hexad suggests the biological interpretation of our ecological statistical mechanics theory for more complex communities.

Figure 4 The GLMY homology dissection of microbial hypernetworks. (A) Homology barcodes (HR) based on positive interaction, negative interaction and mixed (positive and negative) interaction hypernetworks. The homologies are calculated at dimension 1, 2, 3, and 4. (B) Homological networks for mixed positive and negative interactions at dimension 4. (C) Homological networks for negative and mixed interactions at dimension 3, respectively.

Figure 5 The detection of active and passive HOI in a three-species (E-S-P) community. (**A**) Hypernetworks as a collection of nodes (E, S, P), pairwise edges (E-S, S-P, P-E), and HOI edges (SP→E, EP→S, ES→P) under mutualism (black bidirectional arrow line), antagonism (black bidirectional T-shaped line), altruism (black directed arrow line), and aggression (black directed T-shaped line). Red and blue directed arrows represent the promotion and inhibition of active HOI for a focal species, respectively, with the strength of influence proportional to the thickness of lines. (**B**) Time-dependent abundance trajectory (blue line) of each species (E, S, P) observed in the triad decomposed into its independent component (red line) due to this species' intrinsic capacity and dependent component (green line) resulting from the influence of the other two species and their interaction. Black dots denote abundance observations of a species at different time points in the triad, fitted by the miODE of equation (3). (**C**) Driven by active HOI, the abundance of each interactive species is shifted to a new state, which in turn influences the directed interactions of the other pair of species. Passive HOI includes the influence of P on E→S and S→E interactions, the influence of S on E→P and P→E interactions, and the influence of E on S→P and P→S interactions under mutualism, antagonism, altruism, and aggression. In each case, the influence of one species on the second observed in the triad (blue line) is decomposed into the same type of influence assumed to occur in a dyad (red line) and passive HOI curve (green line).

Figure 6 Experimental validation of the statistical hypernetwork model as an ecological statistical mechanics theory. (**A**) Independent growth component curves of each species estimated from two dyads involving this species (thin blue line), in comparison with the fitted growth curve

(thick blue line) of this species' abundance data (blue dots) in its monoculture. (**B**) Independent growth component curves of each species estimated from the triad under different types of pairwise interactions (green, red, purple and orange lines for mutualism, antagonism, altruism, and aggression, respectively), in comparison with the fitted growth curve (blue line) of this species' abundance data (blue dots) in its monoculture. (**C**) Dependent growth component curves of each species affected by its coexisting species estimated from the triad when no third species is assumed to exist, under different types of pairwise interactions (green, red, purple and orange lines for mutualism, antagonism, altruism, and aggression, respectively), in comparison with the same type of dependent growth component curves (blue line) estimated from the dyads.

Figure 7 Structural change of an ecological community over time. Three constituent species (E, S, P) establish a co-occurrence network in state 1. Under active HOI, the community enters state 2, in which new interactive relationships are formed. Newly formed interspecific interactions in turn affect the growth of individual species through passive HOI. The species are then reshuffled to comprise state 3 of the community. This process is iterated to drive the community to diversify and evolve over ecological time. Red and blue arrowed lines represent promotion and inhibition, respectively, with the thickness of lines proportional to the strength of interaction.

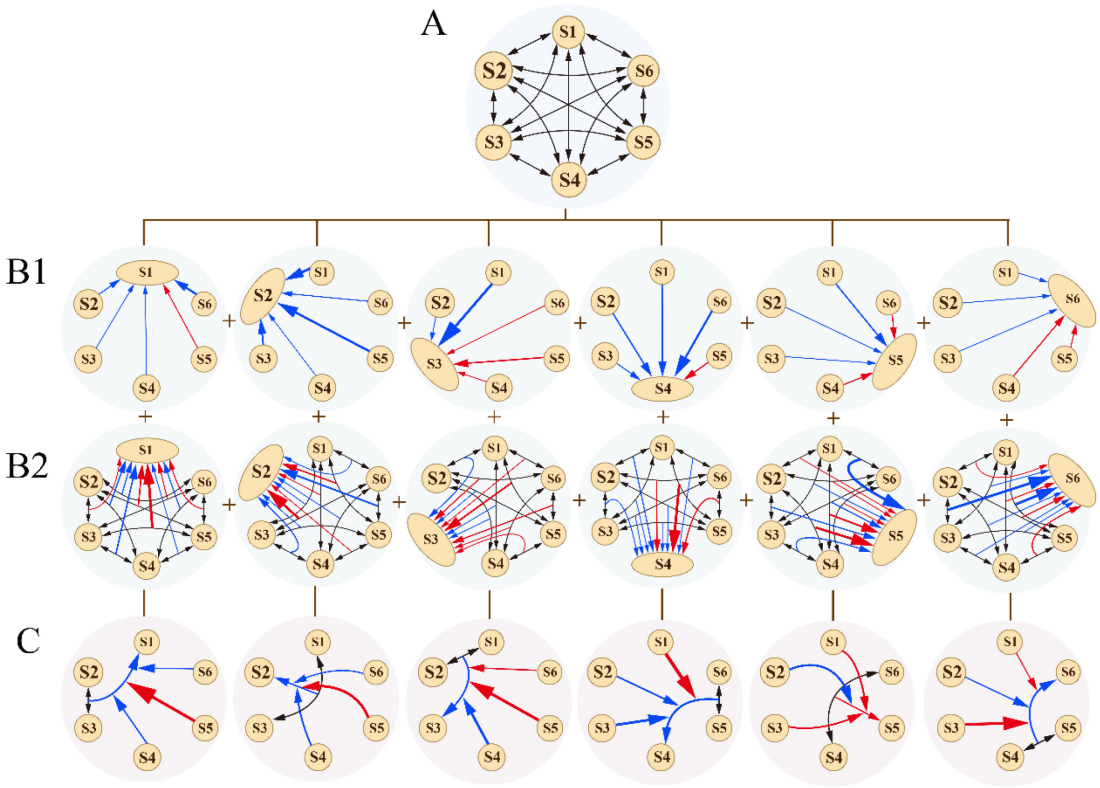

Figure 1

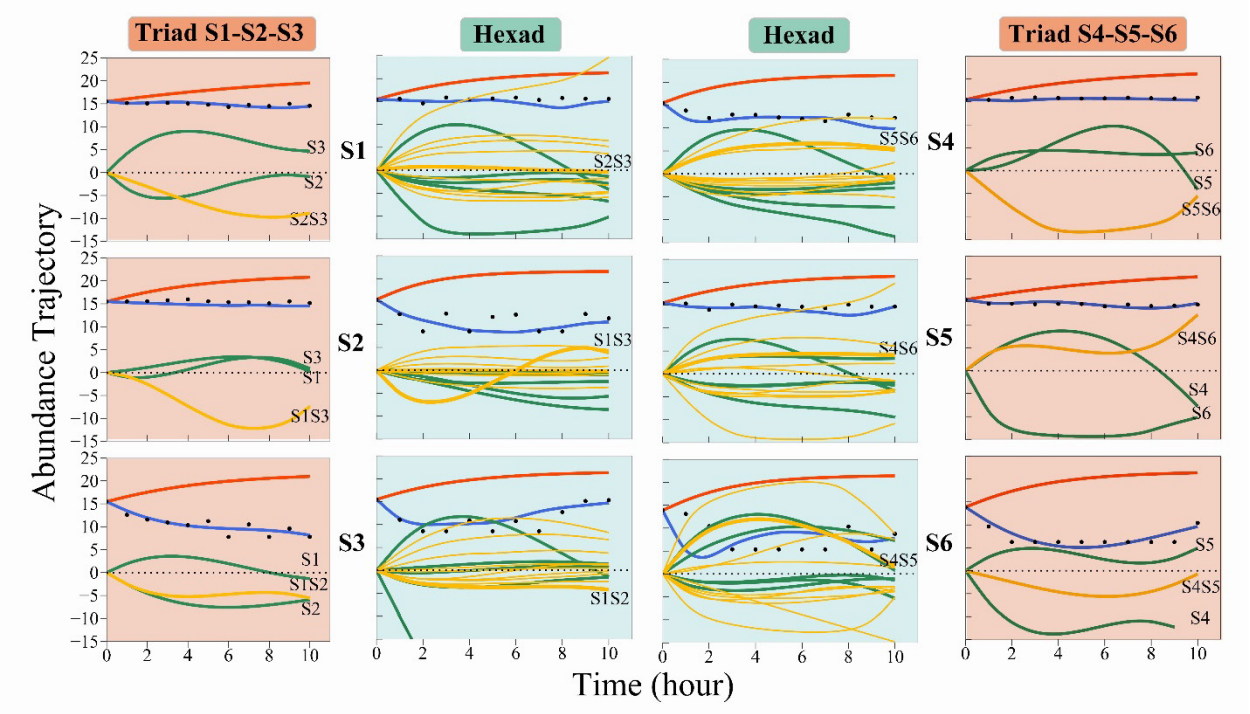
Triad S1-S2-S3
Hexad
Hexad
Triad S4-S5-S6
Abundance Trajectory
Time (hour)
S1
S2
S3
S4
S5
S6
S3
S2
S2S3
S2S3
S1S3
S5S6
S6
S5
S5S6
S3
S1
S1S3
S4S6
S4S6
S4
S6
S1
S1S2
S2
S1S2
S4S5
S4S5
S5
S4S5
S4

Figure 2

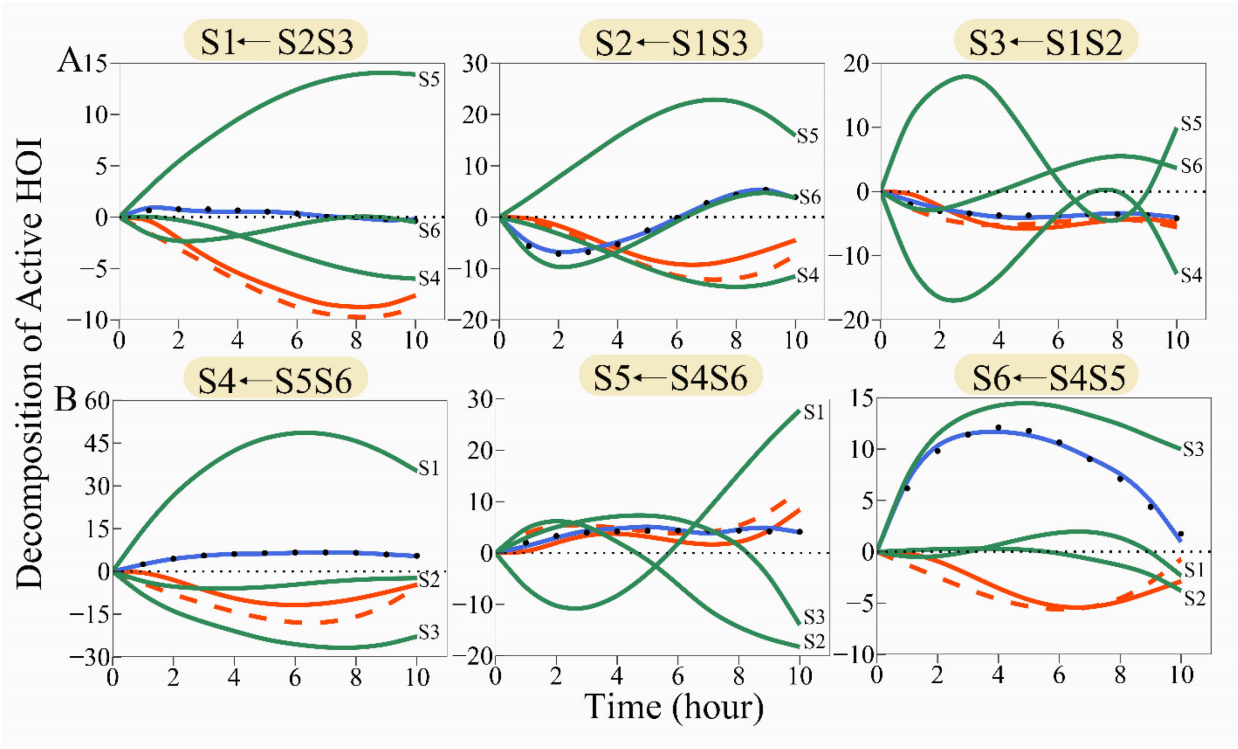
A
B
S1←S2S3
S2←S1S3
S3←S1S2
S4←S5S6
S5←S4S6
S6←S4S5
Decomposition of Active HOI
Time (hour)

Figure 3

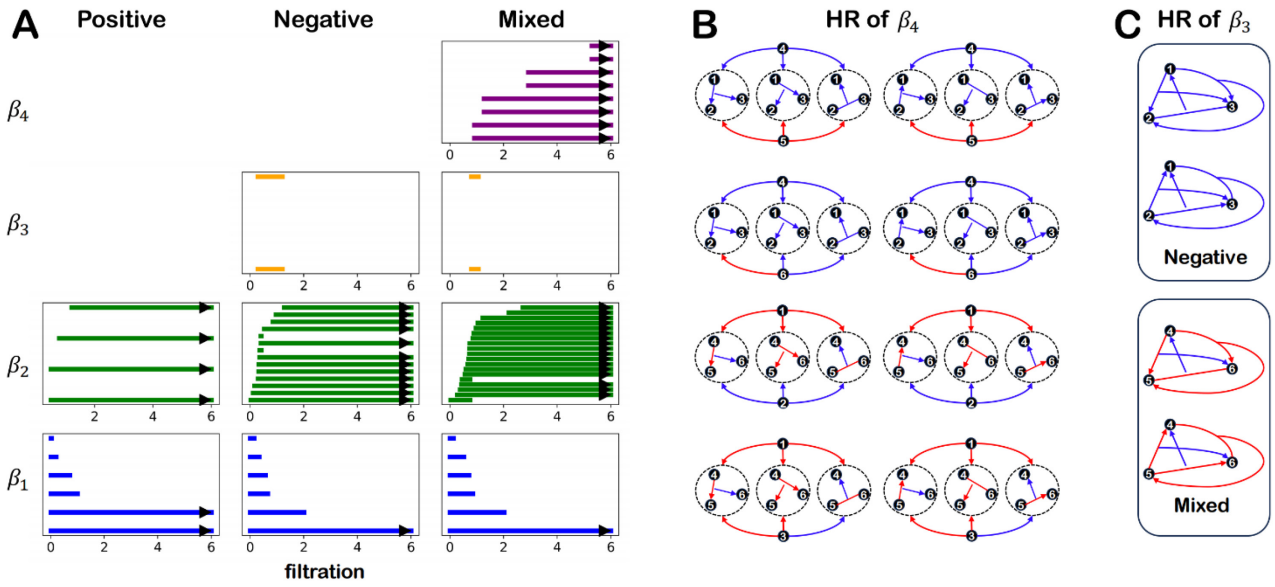
A
Positive
Negative
Mixed
β_4
β_3
β_2
β_1
filtration
B
HR of β_4
C
HR of β_3
Negative
Mixed

Figure 4

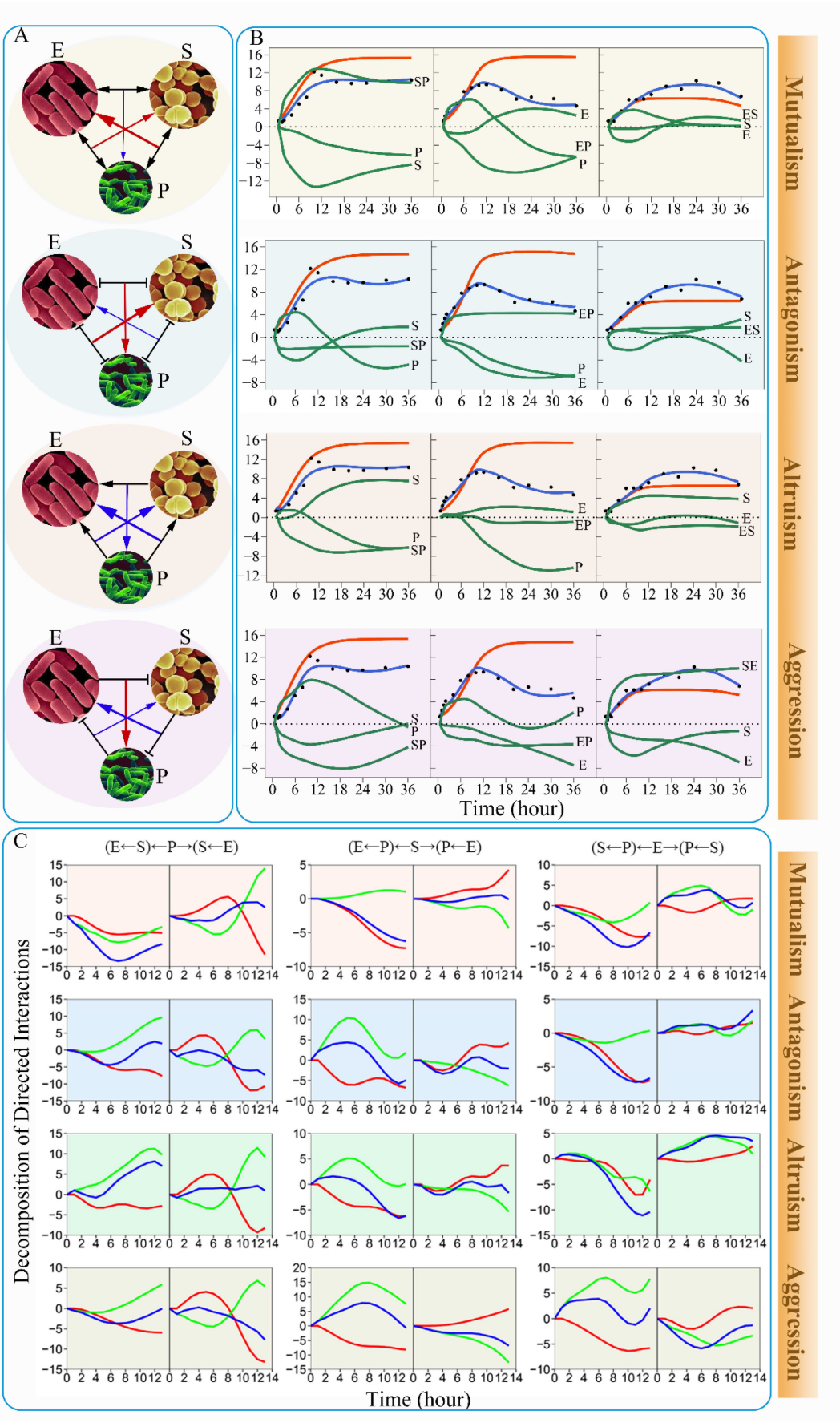
A
E
S
P
B
Mutualism
Antagonism
Altruism
Aggression
Time (hour)
C
(E←S)←P→(S←E)
(E←P)←S→(P←E)
(S←P)←E→(P←S)
Decomposition of Directed Interactions
Time (hour)

Figure 5

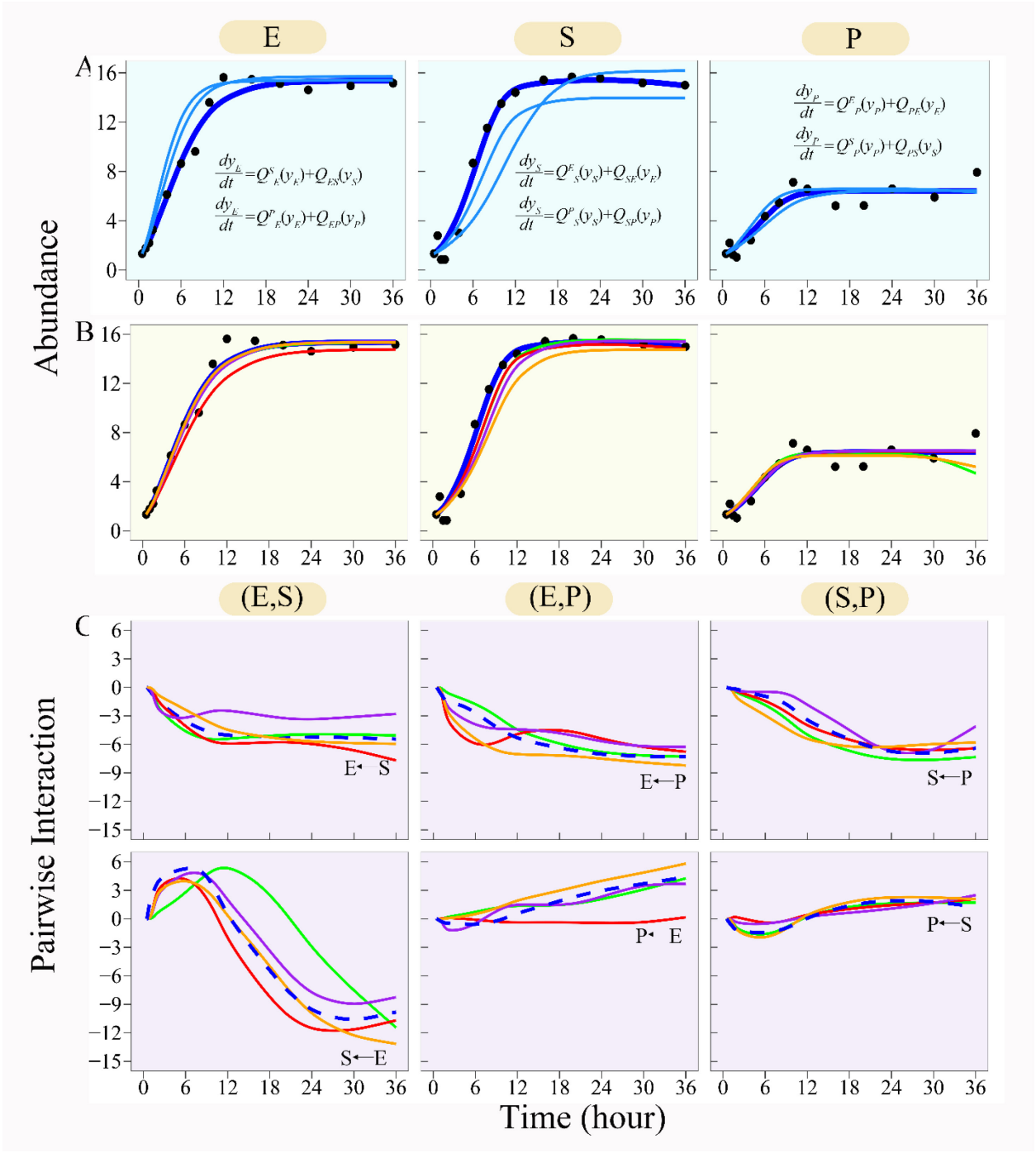
E
S
P
A
B
Abundance
$\frac{dy_E}{dt}=Q^S_E(y_E)+Q_{ES}(y_S)$
$\frac{dy_E}{dt}=Q^P_E(y_E)+Q_{EP}(y_P)$
$\frac{dy_S}{dt}=Q^E_S(y_S)+Q_{SE}(y_E)$
$\frac{dy_S}{dt}=Q^P_S(y_S)+Q_{SP}(y_P)$
$\frac{dy_P}{dt}=Q^E_P(y_P)+Q_{PE}(y_E)$
$\frac{dy_P}{dt}=Q^S_P(y_P)+Q_{PS}(y_S)$
(E,S)
(E,P)
(S,P)
C
Pairwise Interaction
E→S
E←P
S←P
S→E
P→E
P←S
Time (hour)

Figure 6

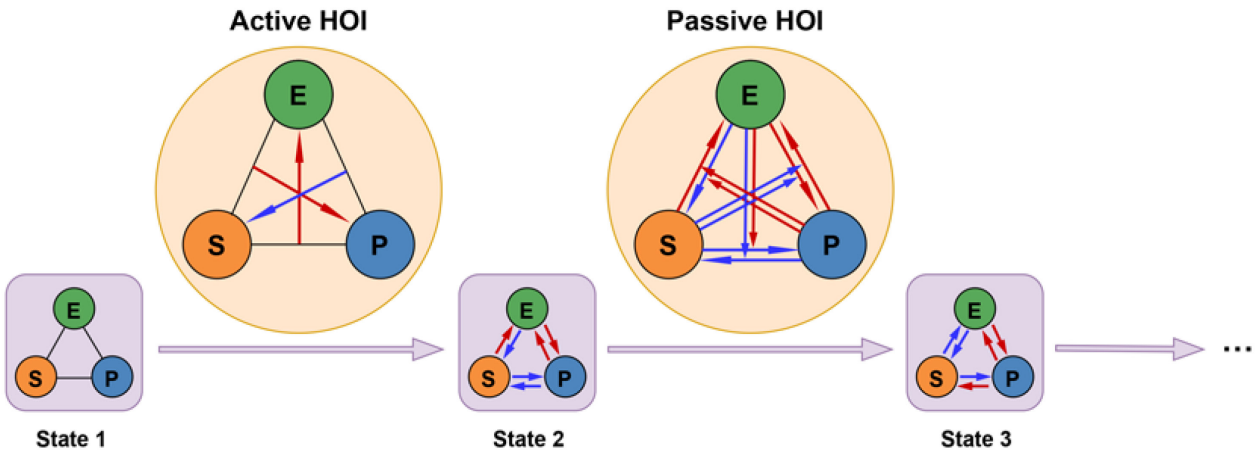

Figure 7